

# Application assessments of concrete piezoelectric smart module in civil engineering

Nan Zhang\*<sup>1</sup> and Huaizhi Su<sup>2a</sup>

<sup>1</sup>*School of Civil and Construction Engineering, Oregon State University, 101 Kearney Hall, Corvallis, OR, USA 97331*

<sup>2</sup>*State Key Laboratory of Hydrology-Water Resources and Hydropower Engineering, Hohai University, Nanjing 210098, China*

(Received August 6, 2016, Revised January 18, 2016, Accepted January 20, 2017)

**Abstract.** Traditional structural dynamic analysis and Structural Health Monitoring (SHM) of large scale concrete civil structures rely on manufactured embedding transducers to obtain structural dynamic properties. However, the embedding of manufactured transducers is very expensive and low efficiency for signal acquisition. In dynamic structural analysis and SHM areas, piezoelectric transducers are more and more popular due to the advantages like quick response, low cost and adaptability to different sizes. In this paper, the applicable feasibility assessment of the designed “artificial” piezoelectric transducers called Concrete Piezoelectric Smart Module (CPSM) in dynamic structural analysis is performed via three major experiments. Experimental Modal Analysis (EMA) based on Ibrahim Time Domain (ITD) Method is applied to experimentally extract modal parameters. Numerical modal analysis by finite element method (FEM) modeling is also performed for comparison. First ten order modal parameters are identified by EMA using CPSMs, PCBs and FEM modeling. Comparisons are made between CPSMs and PCBs, between FEM and CPSMs extracted modal parameters. Results show that Power Spectral Density by CPSMs and PCBs are similar, CPSMs acquired signal amplitudes can be used to predict concrete compressive strength. Modal parameter (natural frequencies) identified from CPSMs acquired signal and PCBs acquired signal are different in a very small range (~3%), and extracted natural frequencies from CPSMs acquired signal and FEM results are in an allowable small range (~5%) as well. Therefore, CPSMs are applicable for signal acquisition of dynamic responses and can be used in dynamic modal analysis, structural health monitoring and related areas.

**Keywords:** modal analysis; power spectral density; structural health monitoring; numerical analysis; ITD

## 1. Introduction

Civil infrastructures (e.g., bridges, buildings) and large scale concrete hydraulic structures (e.g., dams, sluices) have benefits for the nearby communities, the economy as well as the social utilities. Safety and reliability maintaining of the structures for daily usage is significantly important not only for well beings of communities but for the economic benefits (Chang *et al.* 2003). It is necessary to monitor the status of the structures during their operation to guarantee the safety conditions (Su *et al.* 2015, 2016). SHM includes the monitoring of dynamic response measurements from arrays of sensors and transducers distribute all over the structures. Therefore, the quality, sensitivity and accuracy of sensors and transducers have significant effects on monitoring structure operation conditions. Typically, in dam safety monitoring area, sensors like reinforcement meters, osmometers, and joint meters are set up discretely in dam structures, however, these sensors are very expensive and easily broken during the operation. Recently, optical fiber

and piezoelectric transducers are more widely used sensors or transducers (e.g., Tennyson *et al.* 2001, Guo *et al.* 2011, Leung *et al.* 2015, Roy *et al.* 2015, Xu *et al.* 2015). However, optical fiber sensors and piezoelectric sensors used are often stucked to the target structures to collect the signals of the structures under certain vibrations. The sensors used for signal acquisition have three different goals: dynamic modal analysis, electromechanical E/M impedance and wave propagation (Giurgiutiu 2007). The obtained signals are used for dynamic modal parameters extraction and damage detection. Even though the accuracy increases with the using of optical fiber and piezoelectric sensors, the setup and cost should also be taken into consideration. In order to solve this problem, some “artificial” sensors called “smart aggregate” are developed for structural monitoring (Gu *et al.* 2006, Song *et al.* 2007).

The developed “smart aggregates” consist of piezoelectric ceramic patches embedded into concrete with water-proof coating in between, which are used for signal emission and acquisition. The ceramic patches are much cheaper than the manufactures of piezoelectric sensors or transducers but serve as the same function for signal acquisition. One drawback is there will be more noise in the acquired signals.

Sensors and transducers can be used in many Civil Engineering areas, such as damage detection of structures

\*Corresponding author, Ph.D. Student

E-mail: zhangn@oregonstate.edu

<sup>a</sup> Ph.D.

E-mail: su\_huaizhi@hhu.edu.cn

and structural health monitoring. Most of the usages are based on the frequency properties from acquired signals. Based on the acquired signals, some researchers studied the direct changes of structural stiffness due to damage based on Adaptive Least Mean Square filtering theory (Chase *et al.* 2004). Impedance-based health monitoring techniques were applied for damage detections based on the acquisition signals from piezoelectric transducers and sensors (Bahei-El-Din *et al.* 2003; Park *et al.* 2000). Gu *et al.* (2006) designed piezoelectric-based concrete smart aggregates for concrete strength monitoring based on the signal amplitude changes along the concrete early ages and also extend its application on SHM (Song *et al.* 2007). Some researchers studied the development of intelligent being monitored structures (Aktan *et al.* 1997). Dynamic modal analysis (MA) was also applied for damage detections since the magnitude of change in natural frequencies is a function of severity and location of deterioration in structures. Modal analysis method was demonstrated to be effective for skeletal structures (Hearn *et al.* 1991, Clayton *et al.* 2006, Gentile *et al.* 2015, Prashant *et al.* 2015). Modal parameter (modal frequencies, mode shapes, damping ratio) changes based damage detection and structural health monitoring can be a good approach (Chang and Kim 2016). All the presented usages are based on the acquired signals from being detected structures.

Modal parameters will change if there are damages occur in the structures. EMA relies on sensors/transducers to acquire/excite signals from/to the target structures. Thus, the accuracy of modal parameters acquisition can be used to assess the characteristics of transducers and sensors. The following work will focus on (1) frequency comparison between CPSMs acquired and excited signal, (2) Compressive strength prediction of concrete by using CPSMs and (3) the modal parameters extraction through CPSMs acquired signal. CPSMs, which are similar to the designed “smart aggregates” by Song *et al.* (2011), are built with piezoceramic patches embedded in concrete, and RTV silicone as coating as water proof in-between. The concrete mix for constructing CPSMs are similar to the being monitored structures to guarantee homogeneity of the whole system. In the paper, a concrete gravity dam model is poured with three couples of CPSMs being embedded as transducers and sensors (i.e., 6 CPSMs) which being set up at dam toe, heel and crest. Additionally, 6 PCB sensors are set up by gluing on the dam model surface for comparison. For better processing the experiment and avoiding signal refraction and dissipation at the interface between CPSMs and dam section, concrete mixture for CPSMs and dam model are controlled by the similar water-cement-sand ratios under the same temperature. CPSMs are poured first and then embedded in the dam model. The CPSMs-dam model system will be stucked to a shaking table for excitation with white noise. CPSMs and PCB signals will be acquired for modal parameters extraction. For experimental modal analyses, time-domain methods Natural Excitation Technique (NExT) and the Ibrahim Time Domain Technique (ITD) methods are used to obtain modal parameters. For numerical modal analysis, finite element method (FEM) modeling is performed by using ANSYS

14.5. During this procedure, modal parameters extracted through signals acquired from CPSMs and PCBs are analyzed and compared, and the results obtained from FEM and CPSMs are also compared for assessment.

In the paper, signal frequency properties are compared between CPSMs acquired signal and PCB accelerometer signal; concrete compressive strength is indirectly predicted by using CPSMs; the first ten order modal parameters are extracted by experimental analysis. The results show that, PSD of chirp signal and CPSMs acquired signal have similar distributions; a fitting function is made related to CPSMs acquired signal amplitudes and compressive strengths during concrete hydration; and, for experimental modal analysis methods, the modal parameters differences (e.g., natural frequency) between signals acquiring form CPSMs and PCB are very small (~3%); the difference between numerical extracted modal parameters and CPSMs extracted modal parameters are also very small (~5%). The small differences obtaining between two different sensors (i.e., CPSMs and PCBs), between FEM and CPSMs, show that CPSMs can be used as sensors for signal acquisition. As an extension, the CPSMs can thus be used for damage detection and structural health monitoring in Civil Engineering.

## 2. Overview of concrete piezoelectric smart model

CPSMs are the man-made transducer/sensor for the applications on target monitoring structures (see Fig. 1). It is more convenient to set up not only inside the target structures but on the surface. However, PCB transducers can only be set up on the target monitoring structure surface and they are also very expensive. The advantages of CPSMs over PCBs are obvious especially for large scales concrete structure, like dams, bridges and sluices. CPSMs can be built up and embedded in the structures to construct structural health monitoring and damage detection system with much lower expenses. The paper (1) does frequency comparisons between CPSMs acquired and PCB accelerometer acquired signal; (2) uses CPSM to get the signal attenuation function for different frequencies; (3) uses CPSM to estimate the concrete strength along with hydration and (4) analyzes the availability of CPSMs for damage detection and structural health monitoring through modal analysis and uses the modal parameters to evaluate the feasibility of CPSMs in the SHM, damage detection and MA areas.

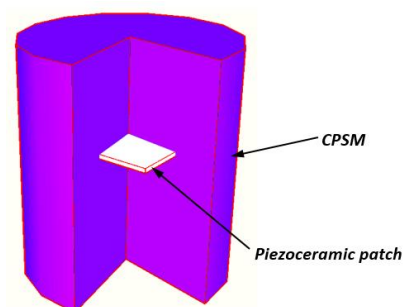


Fig. 1 Diagram of concrete smart piezoelectric model

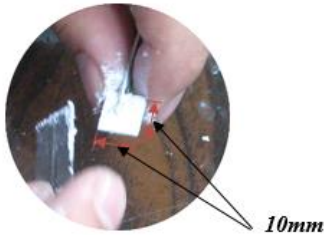


Fig. 2 PZT and coated Silicon

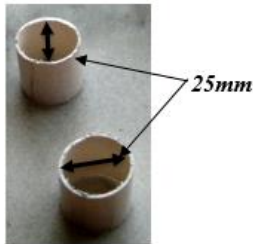


Fig. 3 PVC pile made CPSM molds

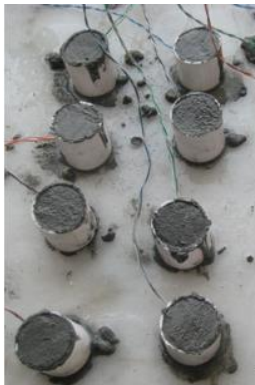


Fig. 4 CPSM after pouring

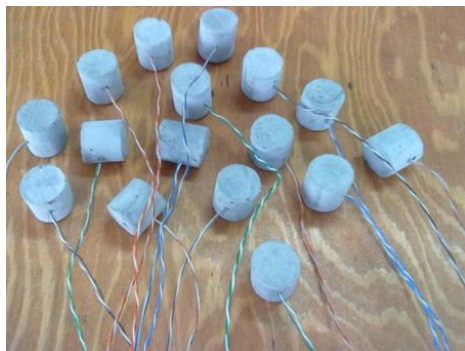


Fig. 5 CPSM ready for application

The embedded Piezoelectric Ceramic (PZT) in the CPSM is selected as MODEL PIC151 made by PCB Inc. Small patches ( $10\text{ mm} \times 10\text{ mm} \times 1\text{ mm}$ ) are cut to meet the requirement of CPSM (Fig. 2). Ethanol is employed to remove the Oxide film before being embedded into the concrete to guarantee the good electric charge transmission

(Su *et al.* 2016). Afterwards, two cables are welded on two surfaces, the joints should be smaller enough to ensure thin waterproof layers. RTC silicone, which has a favorable hardness and damping, is then coated on the surface of the PZT as the waterproof. The molds for pouring concrete are using PVC pipe (see Fig. 3) with an inner diameter of  $\Phi = 25\text{ mm}$ . Additionally, composite is coated on the surfaces for further protection. Concrete will shrink during hydration, stress concentration will thus appear due to the shrinkage stress. The built CPSMs are shown in Fig. 4 as follow. The CPSM ready for application are shown in Fig. 5.

The outer concrete is only for protecting embedded PZT with no carrying pressures applied to the being monitored outside structures. Reinforcements are thus not used during the making of CPSMs. Cement, fine sands and water are only used with a weight ratio of 2.9:2.09:1. Fine materials will reduce the inhomogeneous characteristics of the sample and their stress concentration influences on PZT. The made CPSMs can serve as sensor as well as transducer in Civil Engineering area. The assessment of the built CPSMs on Civil Engineering are presented in the paper as follows.

### 3. Assessment of CPSM in civil engineering applications

Several tests are applied based on CPSM to assess the feasibility and application on the Civil Engineering areas. First, CPSM is used to acquire the signals propagating through concrete generated from wave generator with certain frequency and compare the frequencies of to the original excited signal. Second, large concrete block is poured to qualitatively assess the concrete strength development in the process of hydration. Third, modal analyses result comparison between signals acquired by CPSM and manufactured PCB sensors, between CPSMs and FEM modeling are performed. Meanwhile, the concrete attenuation function is obtained according to the attenuation of signal amplitudes. The being analyzed signal is acquired by digital Signal Processing and Control Engineering (dSPACE) system which is a based on MATLAB/Simulink to achieve Real-Time Interface.

#### 3.1 Frequency comparison

The part is based on the frequency comparisons between signal acquired by CPSMs and signal generated by wave generator. Even though the strength of the signal acquired from CPSMs will decrease during the propagation through concrete, the frequency properties of the signal will remain the same. CPSMs are set up in the concrete blocks shown in Fig. 6 below.

In the experiment, two CPSMs are embedded in the concrete block aligning in same line with certain distance (no matter what the distance it is, just assess the frequency). One side (top) is connected to Wave Generator for signal emitting and the other side (bottom) is connected to dSPACE system for signal acquisition. The emitting signal from Wave Generator is the linear Chirp Signal. Linear

chirp signal sweeps the frequencies from low to high linearly. The sweep frequency in the test is from 10 Hz to 4000 Hz with cyclic duration of 5 seconds. According to Nyquist's theorem, there is no information loss if the sampling frequency is twice of the highest frequency component (Quinquis 2010). The sampling frequency is selected as 40000Hz (ten times of highest frequency) in order not to lose any information. Fig. 7 shows the very initial 0.2 seconds of the total signal.

The basic logic of the comparison is using Fast Fourier Transform (FFT) to extract the frequency characteristics of chirp signal and CPSM acquired signal and to obtain their power spectral densities (PSD). A random signal usually has finite power that can be characterized by an average power spectral density which is considered as power spectral density (Stoica and Moses 2005). The PSD curves represent the continuous probability density function of the responses. The comparisons of PSDs will be made for both excited and acquired signals and whereby to assess the feasibility of CPSMs in the applications for Civil Engineering. FFT converts the signal from time domain to frequency domain (Brigham 1974). FFT is a tool to perform signal analysis such as PSD and filter simulations. The PSD of the excited Chirp Signal are shown in Fig. 8.

A one-side Power Spectral Density contains the total power of the signal in the frequency interval from DC to half of the Nyquist rate. However, double sides PSD contains all the power of the signal in the frequency interval from DC to the Nyquist rate.

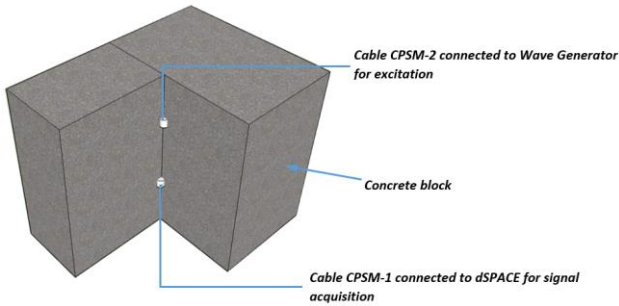


Fig. 6 Diagram of concrete block and embedded CPSMs

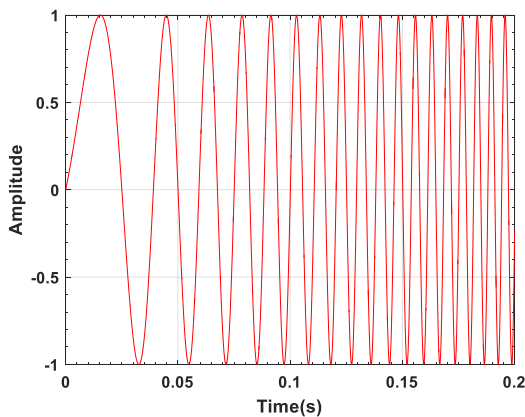
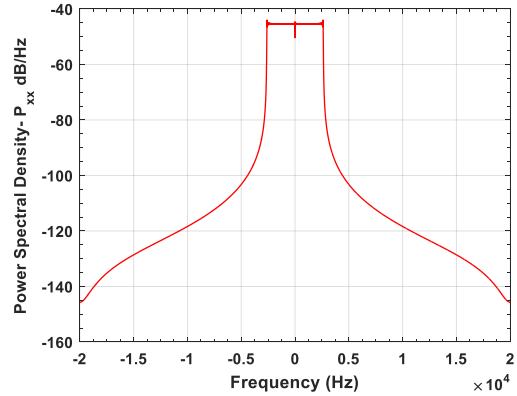
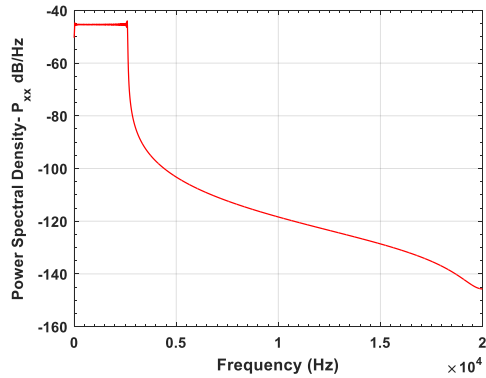


Fig. 7 Excited chirp signal of CPSM-1



(a) Double sided Power Spectral Density



(b) One side Power Spectral Density

Fig. 8 PSD of wave generator excited chirp signal

The magnitude of emission signal is 1, however, the value decreases to 0.06 when acquiring it due to the damping during propagation (See Fig. 9) between the transmitted distance between two CPSMs (PZT patches) and piezoelectric effects of the selected PZT patches.

Noise inside CPSM acquired signal is filtered by low-pass filter with Kaiser Window. The cutoff frequency is set up as the maximum signal frequency as 4000 Hz. The original and filtered signal in the very beginning 0.5s is shown in Fig. 10.

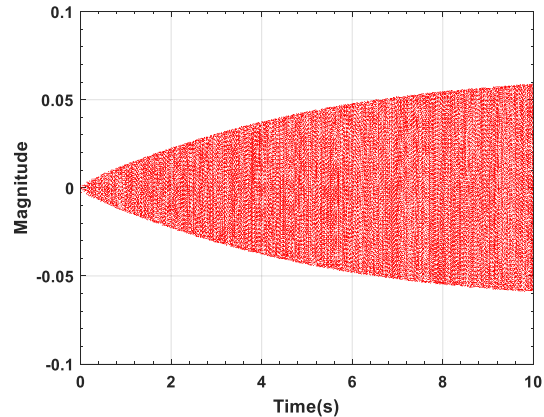


Fig. 9 CPSM acquired chirp signal

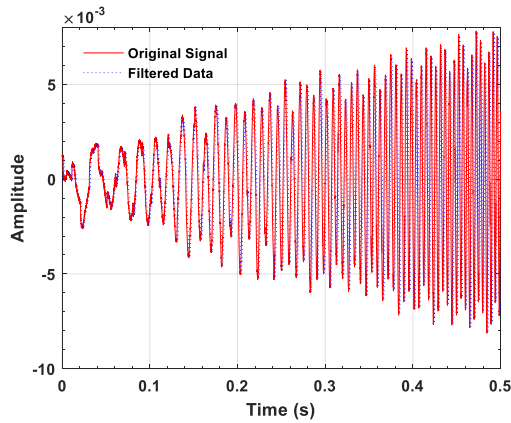
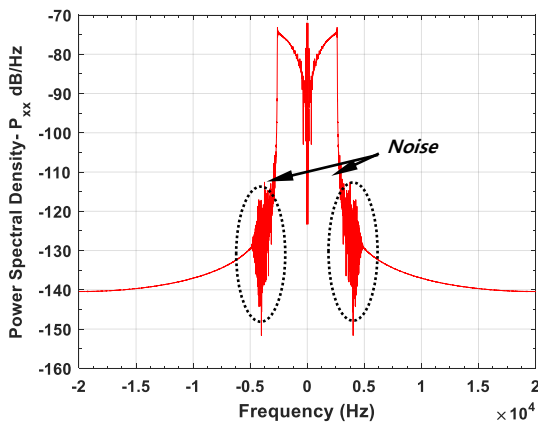
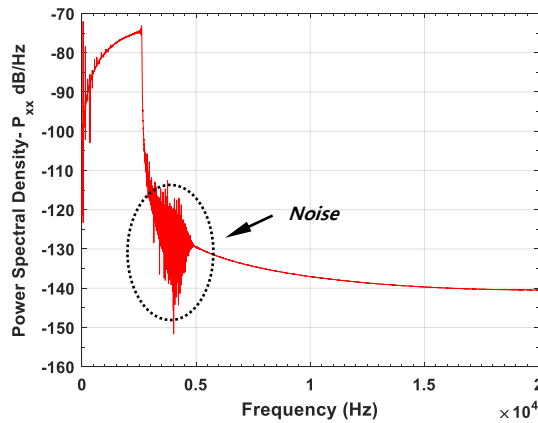


Fig. 10 Filtered CPSM signal



(a) Double sided Power Spectral Density



(b) One side Power Spectral Density

Fig. 11 PSD of CPSM acquired chirp signal

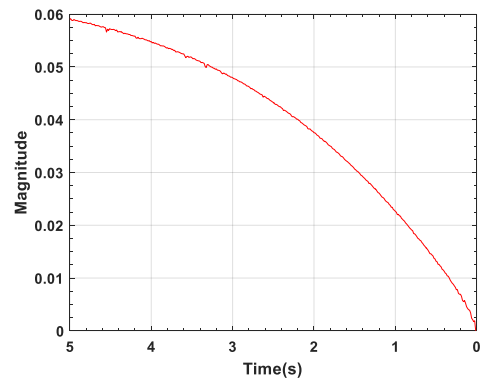
Through the comparison of Figs. 8 and 11, the PSD ranging from 0 Hz to 20000 Hz have the similar distributions even the magnitudes between them are not exactly the same. The frequencies with higher power spectral densities for both chirp signal and CPSM acquired signal are in the same range. Different from the PSD of chirp signal, the peak PSD values for CPSM acquired signal are smaller. The reason may be explained by considering

that the noise is also acquired by CPSM. The dash ellipses in Fig. 11 mark the noise that have not been fully filtered when remain the CPSM acquired chirp signal. The noise might make the PSD magnitude for CPSM acquired signal a little smaller. Noises disperse the PSD and make the PSD values smaller corresponding to the original excited signal. Additionally, signal attenuates in the propagation from one CPSM to the other. Coated silicon and the interface between concrete and PZT patches, interface between CPSM and concrete block can attenuate the acquired signal as well.

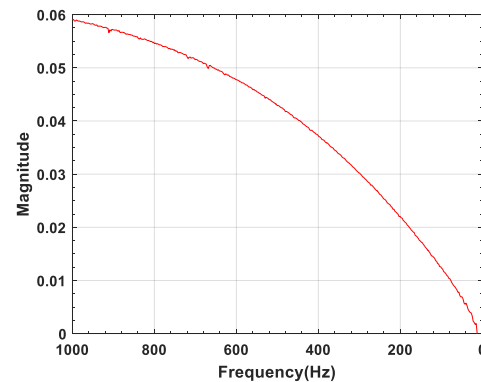
### 3.2 Attenuation function

The two CPSMs embedded in the concrete block are fixed during signal exciting and acquisition. The frequencies sweep from 10Hz to 1000Hz. Signal will attenuate due to the distances of signal propagating. And the higher the frequency, the more loss the amplitude during propagation. Typically, in a certain range, the lower the frequency, the higher the attenuation will be. The attenuation curve for the studied CPSM is in shown in Fig. 12. The attenuation curve can also be shown as magnitude versus frequencies since the chirp signal is linearly swept, See Fig. 12.

The excited signal has a magnitude of 1 while the acquired signal has a magnitude of 0.06 which is set as the initial value for evaluation of attenuation along with frequencies. The magnitude when the excited frequency equals to 10 Hz is 0.0012.



(a) Magnitude (mV) vs. Time



(b) Magnitude (mV) vs. Frequency

Fig. 12 Attenuation curve

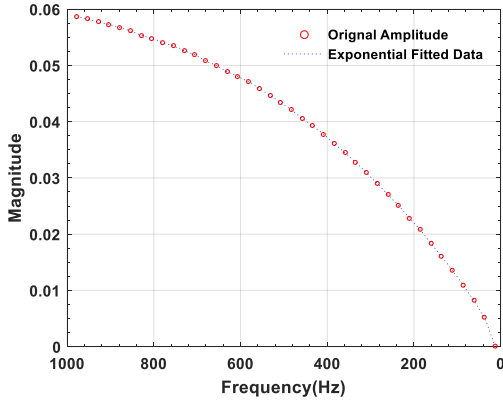


Fig. 13 Amplitude based attenuation function along with different sweeping frequencies

The amplitude attenuation function along with sweeping frequencies is fitted to be the addition of two exponential functions as Eq. (1).

$$A(f) = 0.1165e^{-0.00027f} - 0.1162e^{-0.0014f} \quad (1)$$

where  $A$  is amplitude which is assumed to be a function of frequency,  $f$  is sweep frequency. Exponential fitting can suitably fit the dispersed amplitude data. 0.0065 and -0.1162 are considered the un-attenuated amplitude of the signal at certain location. -0.00027 and -0.0014 are attenuation coefficients along with different sweep frequencies. The units of attenuation coefficients are nepers/Hz if the built CPSMs are regulated.

### 3.3 Concrete strength estimation during hydration

Hydration heat of large-scale concrete will influence the concrete strength due to the thermal expansion and contraction. The excited CPSM emits compression waves and the acquired CPSM acquires the compression wave as digital signal. Compression waves transmitted in the media will attenuate as the distance increases as mentioned above. The compression wave is assumed to be one-dimensionally transmitted in the media (See Fig. 14). The wave propagation equation is shown in Eq. (2).

$$A \frac{\partial \sigma}{\partial z} dz + A\rho \frac{\partial^2 u}{\partial t^2} = 0 \quad (2)$$

where  $\sigma$  is axial stress,  $u$  is axial displacement,  $A$  is the unit section area,  $\rho$  is concrete density,  $A \frac{\partial \sigma}{\partial z}$  is the unite stress difference,  $A\rho \frac{\partial^2 u}{\partial t^2}$  is inertial force.

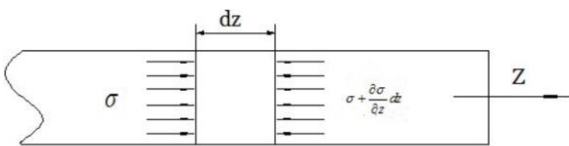


Fig. 14 Force condition of one-dimensional structure

Concrete hydration at very early stage has a strong viscoelasticity. The concrete strength at beginning are very small, however, compressive strength at 7 days is approximately 75% of the strength at 28 days (Haranki 2009). Concrete after approximately 7 days can be assumed as elasticity (Bernard *et al.* 2003). Regardless the influence of strain rate,  $E$  is Young's Modulus of concrete,  $\varepsilon$  is axial strain. The relationship between stress and strain is shown in Eq. (3)

$$\sigma = E\varepsilon = -E \frac{\partial u}{\partial z} \quad (3)$$

substituting Eq. (3) to (2)

$$\frac{\partial^2 u}{\partial z^2} = \frac{1}{c_b^2} \frac{\partial^2 u}{\partial t^2} \quad (c_b^2 = \frac{E}{\rho}) \quad (4)$$

The power of simple harmonic wave in a certain duration can be denoted in Eq. (5) as follow

$$p = \frac{EM^2\omega^2}{2c_b} = \frac{\sqrt{E\rho}M^2\omega^2}{2} \quad (5)$$

where  $p$  is the power of harmonic wave,  $M$  is the amplitude of the harmonic wave,  $\omega$  is angular frequency. Harmonic wave amplitude can be denoted as Eq. (6).

$$M = \left( \frac{1}{\omega} \right) \left( \frac{4p^2}{E\rho} \right)^{\frac{1}{4}} \quad (6)$$

Eq. (6) shows that wave amplitude  $M$  is a function of angular frequency  $\omega$ , power of wave  $p$ , medium density  $\rho$  and Young's modulus  $E$ . Therefore, when  $\omega$ ,  $p$  and  $\rho$  are kept constant, wave amplitude  $M$  is exponentially correlated to Young's modulus of the medium (Achenbach 2012). Young's modulus of concrete has been reported to have a strong relationship with compressive strength by a lot of researcher or institutes (e.g., Architectural Institute of Japan 1985, Tomosawa and Noguchi 1993, Eurocode 2 2004, Noguchi *et al.* 2009). The trend or pattern of concrete strength during hydration can thus be estimated by monitoring the amplitudes of harmonic wave.

A series of tests are designed based on the theory. The same as frequency comparison, wave generator is also employed to generate the signals to excite one CPSM to emit compression waves into the concrete, Oscilloscope is connected to the other CPSM to monitor acquired waves (signals) and record the corresponding signal amplitudes.

The system diagram is shown in Fig. 15. Acquired signal amplitudes are monitored and recorded for 12 different time spots during concrete hydration period. Meanwhile, Compressive Strength of Cement Concrete Cubes tests are also designed to obtain the compressive strength at the corresponding time spots. Thus, acquired signal amplitudes and corresponding concrete compressive strengths, at different times, are recorded for further numerical analysis.

Compressive strength, tensile strength and shear strength are three different characterizations of concrete strength. During operation, plain concrete mainly withstand

compression and shearing. The tensile strength of which is barely small which will not as a pivot aspect. Additionally, compressive test is easy to be applied in the laboratory. The paper will present a series of compressive strength of cement concrete cube tests to obtain compressive strength of the concrete in different times.

For Compressive Strength of Cement Concrete Cubes tests, 36 cement cubes (12 groups) are poured for testing to obtain concrete compressive strengths. The measured compressive strengths of the measured 12 different time compressive strengths are shown in Table 1 and Fig. 18.

Corresponding to the obtained compressive strengths of the concrete in different time spots, CPSM acquired signal amplitudes are also recorded. Three couples of CPSMs are embedded into the concrete block. Data is recorded in 12 hours' interval (8:00 AM and 8:00 PM) each day for 28 days and average the two data as the amplitude of this day. The recorded data is shown in Fig. 19.

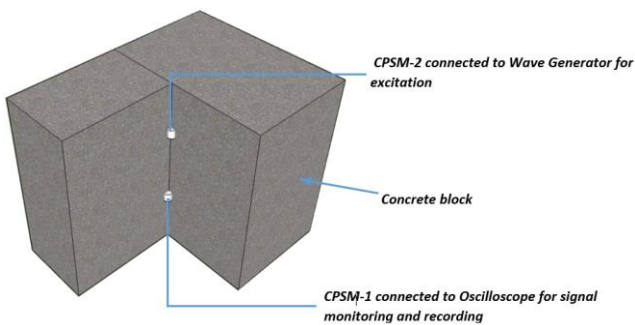


Fig. 15 Concrete strength monitoring during hydration



Fig. 16 Mold for concrete pouring

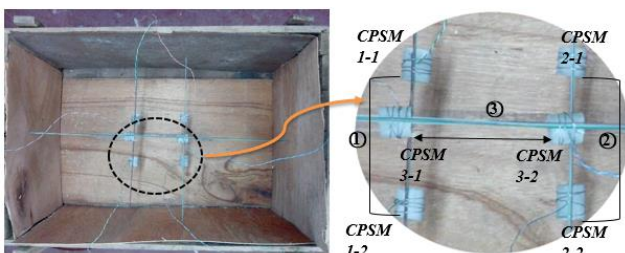


Fig. 17 CPSM set-up in the mold

It is obvious that the magnitudes in the first 7 days is increasing which seems conflict the theoretical in Eq. (6). The reason is that the damping in the very early age is very high. Concrete in the first 7 days are highly viscoelasticity, it means the compressive stress is not linearly related to the strain. Eq. (6) is not applicable for viscoelastic materials.

The concrete is viscous at very beginning. Compressive waves will be highly attenuated during propagation. As time goes on, concrete starts to get solidified. The damping will decrease and wave amplitude will increase. When the damping changes are small enough, the wave amplitude starts to decrease. Signal energy losses during emission.

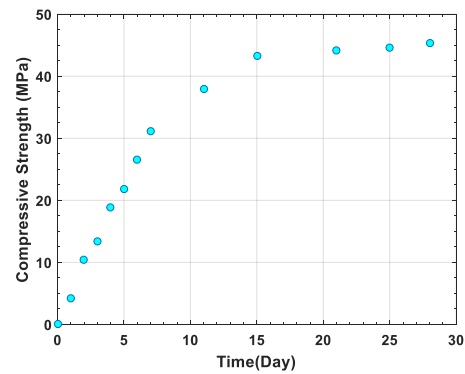


Fig. 18 Compressive Strength development vs. Time

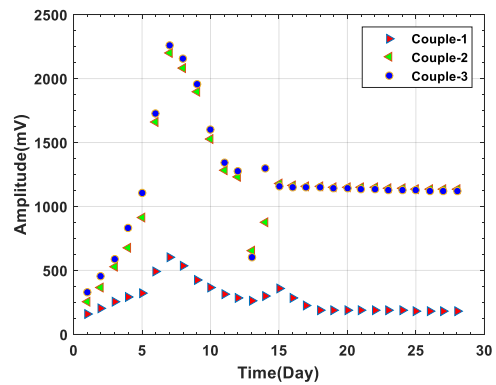


Fig. 19 Signal Amplitudes vs. Time

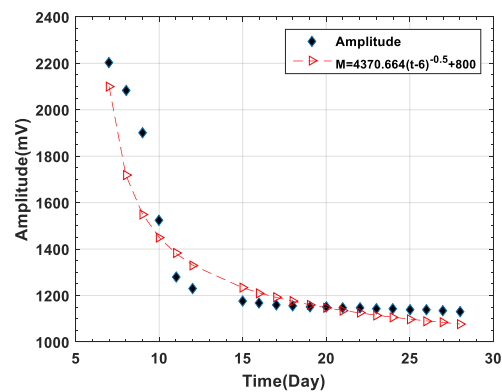


Fig. 20 Signal Amplitude Develops with Time

Table 1 Concrete compressive strength

Day	1	2	3	4	5	6	7	11	15	21	25	28
Compressive Strength (MPa)	4.2	10.4	13.4	18.9	21.8	26.5	31.1	38	43.3	44.1	44.6	45.3

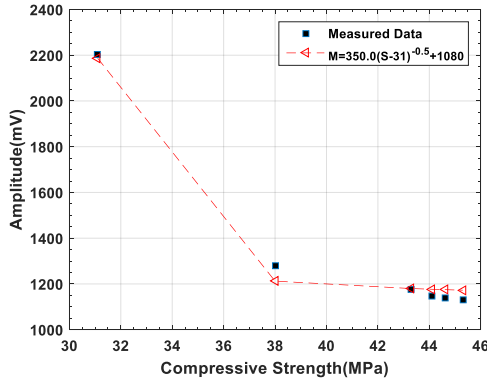


Fig. 21 Signal Amplitudes vs. Compressive Strength

After 7 days hydration, signal amplitudes decrease along with hydration. The analysis data is based on the signal amplitudes between 7- 28 days. The figure (Fig. 20) below shows the root square fitting function of the compressive strength between 7-28 days. The function agrees at earlier stage (from 7-17days), after that the deviations are turned to be larger.

The signal amplitudes during concrete hydration has the relationship of  $M = m(t - n)^{-\frac{1}{2}} + C$  in which n is related to the first effective data. C=800 is related to the close-final stage signal amplitude. The results may be changing varies with the PZT patch characteristics.

If only picking up 7th, 11th, 15th, 21st, 25th and 28th day compressive strength data and the corresponding acquired signal amplitudes of couple 2 and fitting them to a root square function which is shown in Fig. 21, the fitting function of signal amplitudes and compressive strength has the relationship of Eq. (7).

$$M = \alpha(S - \beta)^{-\frac{1}{2}} + C \quad (7)$$

where  $\alpha$  is the coefficient,  $\beta$  is the initial effective compressive strength, C is constant related to the acquired signal amplitude.

The coefficient for couple 2 is  $\alpha = 350.0$ ,  $\beta = 31 \text{ MPa}$  and C=1080 mV. If go back to Eq. (5), the coefficient  $\alpha \propto \frac{2p}{\omega_r \sqrt{\rho}}$  is universal for all the three couples.

### 3.4 Modal analysis

Structures will endure seismic loading which will result in cracks and influence the structural stabilities. Structures need to be monitored to ensure their stabilities for daily use. In the construction, embedding typically manufactured sensors into the target structures will be costly. The CPSM

built in this study will be assessed via dynamic analysis. In order to evaluate the performance of CPSM, one concrete dam model is built. The PCB accelerometers are stucked to the model, and finite element method is applied for comparison. The layout of CPSMs and PCB sensors are shown in the following Fig. 22.

#### 3.4.1 Experimental modal analysis (EMA)

The dam module is placing on a shaking table. PCB accelerometer is manufactured with certain correction for signal acquisition which can accurately acquire the signal acceleration as well as the frequency information. However, the built CPSM can only get the non-regulation signal with the same frequency information as manufactured PCB accelerometer. After being filtered, the signal obtained by both PCB and CPSMs can be used to do structural dynamic modal analysis. The monitoring process is shown in Fig. 23 below.

Experimental modal analysis in the study is based on the Ibrahim Time Domain Technique (ITD) which is put forward by Ibrahim and Mikulcik (1973). The ITD method uses structural free response data to construct two response matrices with a certain time delay between them. The delay relationship is used to form an eigenvalue problem. All the natural frequencies, damping factors and models can be extracted by solving the problem.

Consider a multi DOF system as Eq. (8) as follow.

$$M\ddot{u}(t) + C\dot{u}(t) + Ku(t) = F(t) \quad (8)$$

where  $u(t)$  is the vector of displacements at time t. F(t) is the vector of forces at each time interval, M, C and K are the mass, damping and stiffness matrices respectively. If the excitation is white noise, F(t) above is equal to 0.

The solution of Eq. (8) can be denoted as Eq. (9) in the following

$$u(t) = [\varphi] \{e^{st}\} \quad (9)$$

where  $[\varphi]$  is Eigen-matrix,  $e^{st} = e^{s_1 t}, e^{s_2 t}, \dots, e^{s_{2N} t}$  are the eigenvalues of the structure, N is degree of freedom. Eqs. (8) and (9) can be solved as Eq. (10).

$$(s^2 [M] + s[C] + [K])[\varphi] = 0 \quad (10)$$

For the un-damping linear system, Eq. (10) has the relationship as Eq. (11) as follow.

$$\begin{cases} s_r = -\xi_r \omega_r + j\omega_r \sqrt{1 - \xi_r^2} \\ s_r^* = -\xi_r \omega_r - j\omega_r \sqrt{1 - \xi_r^2} \end{cases} \quad (11)$$

where  $\omega_r$  is  $r$ th order natural frequency,  $\xi_r$  is the corresponding damping ratio. The vibration response at  $i$ th point at  $t_k$  can be denoted as a set as Eq. (12).

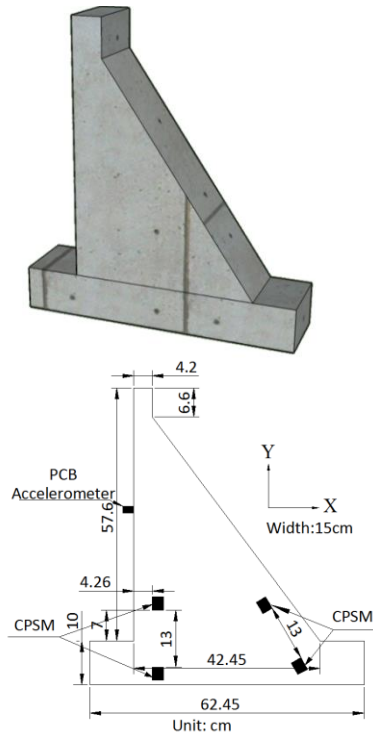


Fig. 22 Concrete dam section, CPSM and PCB accelerometer layout diagram

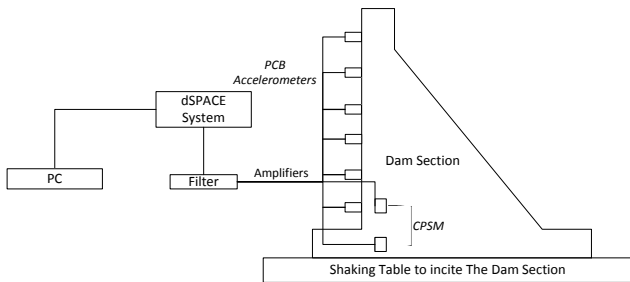


Fig. 23 Monitoring process and the Setup

$$u_i(t_k) = \sum_{r=1}^N \left( \varphi_{ir} e^{s_r t_k} + \varphi_{ir}^* e^{s_r^* t_k} \right) = \sum_{r=1}^M \varphi_{ir} e^{s_r t_k} \quad (12)$$

where  $M = 2N$ ,  $\varphi_{ir}$  is  $i$ th component of  $r$ th order model matrix.

If the measured point is much less than the twice of systematic degree of freedom, virtual point should be constructed by using delay method. The delay should be the integer multiples of  $\Delta t$ . The response is thus shown in Eq. (13).

$$\begin{cases} \delta_{i+n} = x_i(t_k + \Delta t) \\ \delta_{i+2n} = x_i(t_k + 2\Delta t) \\ \vdots \end{cases} \quad (13)$$

The response matrix  $[\Delta]_{M \times L}$  built up by free vibration response of  $M$  measuring points in  $L$  different time as Eq. (14).

$$[\Delta]_{M \times L} = [\Phi]_{M \times M} [\Lambda]_{M \times L} \quad (14)$$

After  $\Delta t$  delay, the response matrix is shown in Eq. (15).

$$[\tilde{\Delta}]_{M \times L} = [\tilde{\Phi}]_{M \times M} [\Lambda]_{M \times L} \quad (15)$$

where  $[\tilde{\Phi}]_{M \times M} = [\Phi]_{M \times M} [\alpha]_{M \times M}$ .

Eq. (16) can be derived by substituting Eq. (14) into (15) as follow.

$$[A][\Phi] = [\Phi][\alpha] \quad (16)$$

where  $[A][\Delta] = [\tilde{\Delta}]$  in which  $[A]$  is the least-square solution. Two Pseudo-inverse solution of  $[A]$  are shown in Eqs. (17) and (18) as

$$[A] = [\tilde{\Delta}][\Delta]^T \left( [\Delta][\Delta]^T \right)^{-1} \quad (17)$$

$$[A] = [\tilde{\Delta}][\tilde{\Delta}]^T \left( [\Delta][\tilde{\Delta}]^T \right)^{-1} \quad (18)$$

The  $r$ th order eigenvalue of  $[A]$  is  $e^{s_r \Delta t}$ . Let the solved eigenvalue  $V_r$  satisfied the following Eq. (19).

$$V_r = e^{s_r \Delta t} = e^{\left( -\xi_r \omega_r + j \omega_r \sqrt{1 - \xi_r^2} \right) \Delta t} \quad (19)$$

The modal frequency  $\omega_r$  and damping ratio can thus be calculated as Eqs. (20) and (21).

$$\omega_r = \frac{|\ln V_r|}{\Delta t} \quad (20)$$

$$\xi_r = \sqrt{\frac{1}{1 + \left( \frac{\text{Im}(\ln V_r)}{\text{Re}(\ln V_r)} \right)^2}} \quad (21)$$

The experimental equipment is shown in Fig. 24. Gravity dam section is placed on a shaking table. Dam section is glued to the shaking table with CPSMs are embedded in the dam section.

White noise with excitation frequency from 100 Hz to 2000 Hz of various equivalent accelerations is used in the test. In the modal analysis, the signal acquired by CPSM and PCB accelerometer are obtained under the excited equivalent frequency equals to 2.0 g. Signal are acquired by dSPACE system with a sampling frequency of 4000 Hz, according to Nyquist theorem. The excitation direction is perpendicular to dam axial, horizontally shown in Fig. 25.

The paper takes signals acquired from CPSM, PCB accelerometer for experimental modal analysis, comparable analysis and assesses the feasibilities of CPSM in structural monitoring analysis.



Fig. 24 Equipment setup

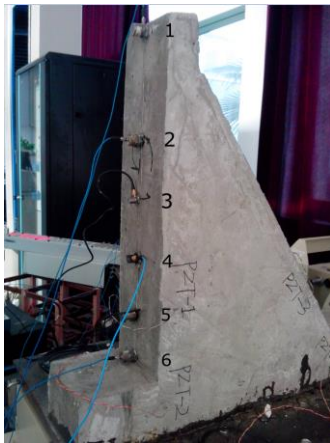


Fig. 25 PCB setup diagram

For the multi measured points’ modal analysis, one reference point need to be selected. Before being used ITD modal analysis, cross power spectral density of two selected measured points are obtained. The modal parameters identification is based on the obtained cross power spectral density. For modal analysis using CPSM, #2 CPSM point (See Fig. 24) is selected as the reference point. The cross power spectral density between #2 CPSM and #1 CPSM is shown in Fig. 26(a) as follow.

The Cross Power Spectral Density is used as the input for ITD modal analysis. The Impulse Response Function of the input Cross Power Spectral Density is in Fig. 27(a) below.

If the same processes are applied to the signal acquired by PCB accelerometer, the Cross Power Spectral Density and Impulse Response Function of it are shown in Figs. 26(b) and 27(b). Cross power spectral density (cross-PSD) is allowed to determine the relationship between two signals as a function of frequency (Zhang and Jia 2005). Cross power spectral density for signals from CPSM and PCB accelerometers are similar. It means the relationships between two CPSMs and two PCB accelerometers are similar. Amplitudes from PCB accelerometers are a little bit larger can be explained by considering damping of coating on PZT patches. Impulse response function is the response of any dynamic systems from external change. Same as cross-PSD, the amplitude is a little bit larger.

For PCB acquired signal based modal analysis, point #1 is selected as reference point. The cross power spectral density is obtained between #1 and #3. Since the dam section is a whole block, wherever the points being selected does not influence the identified results. The first ten order modal parameters are extracted based on PCB acquired and CPSM acquired signals by using ITD modal analysis. The results are shown in Table 2.

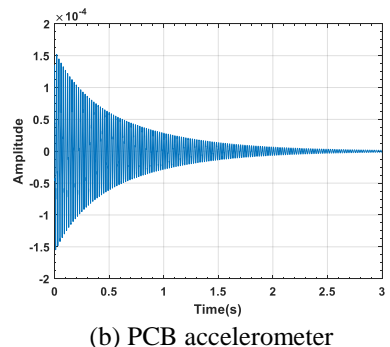
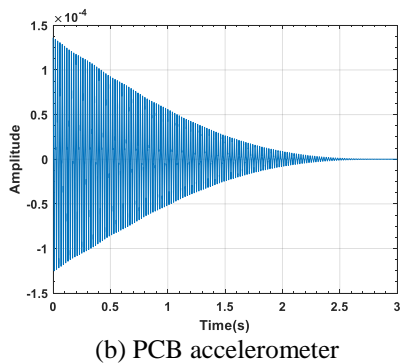
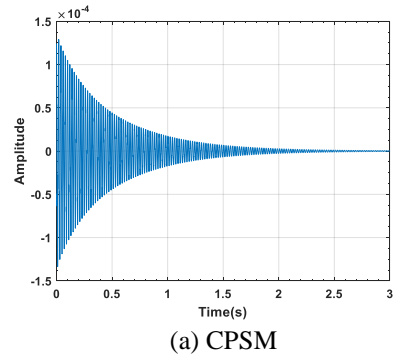
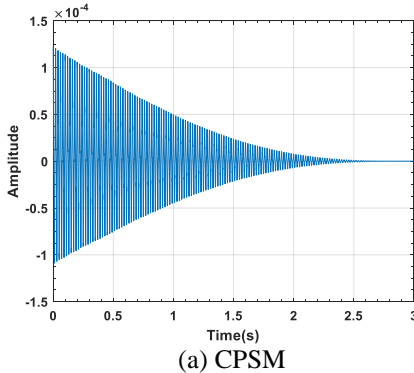


Fig. 26 Cross Power Spectral Density

Fig. 27 Impulse Response Function

### 3.4.2 Numerical modal analysis

Finite element method (FEM) modeling is used in this part to do the modal analysis to compare with experimental modal analyses based on both PCBs and CPSMs. The dam section finite element model is constructed in ANSYS 14.5 with the exactly the same dimensions and material properties as being used for experimental modal analysis. Young's modulus of the concrete is obtained by using rebound hammer as 14.29 GPa, the density of the concrete is measured as 2100 kg/m<sup>3</sup>, and Poisson's ratio is set as 0.30. The dam model is meshed by 14630 hexahedral elements shown in Fig. 28. The degree of freedom (DOF) is set as zero on the bottom surface to model the experimental tests, in which the dam section is stuck to the shaking table. Numerical modal analysis by FEM modeling in the aid of ANSYS 14.5 extracts the first ten order modal frequencies shown in Table 2 as follow. Modal frequencies can be obtained directly from ANSYS post possessing. The first ten order frequencies extracted from ANSYS are shown in Table 2. The displacement vector contour images of all the nodes under first four order natural frequencies are shown in Fig. 29.

The results in Table 2 shows that the natural frequencies extracted from CPSM acquired signal have small relative errors (<3%) in the first 10 orders except 4th, 5th and 10th. The natural frequencies identified from CPSM are acceptable. However, the differences between CPSMs and numerical results are larger (~5%). The reason might be explained that rebound hammer will not give a very accurate Young's modulus which is very sensitive for the modal parameters.

Fig. 30 shows the power spectral density of signals acquired by both PCB (left) and CPSM (right). The comb-like peak values are corresponding to different orders natural frequencies. The manually-manufactured CPSM can extract the frequency properties as regulated PCB accelerometer. The built CPSM and its application can thus be verified and evaluated.

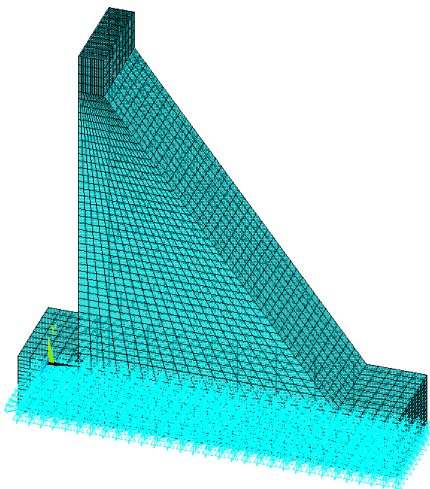


Fig. 28 FEM meshing of dam section

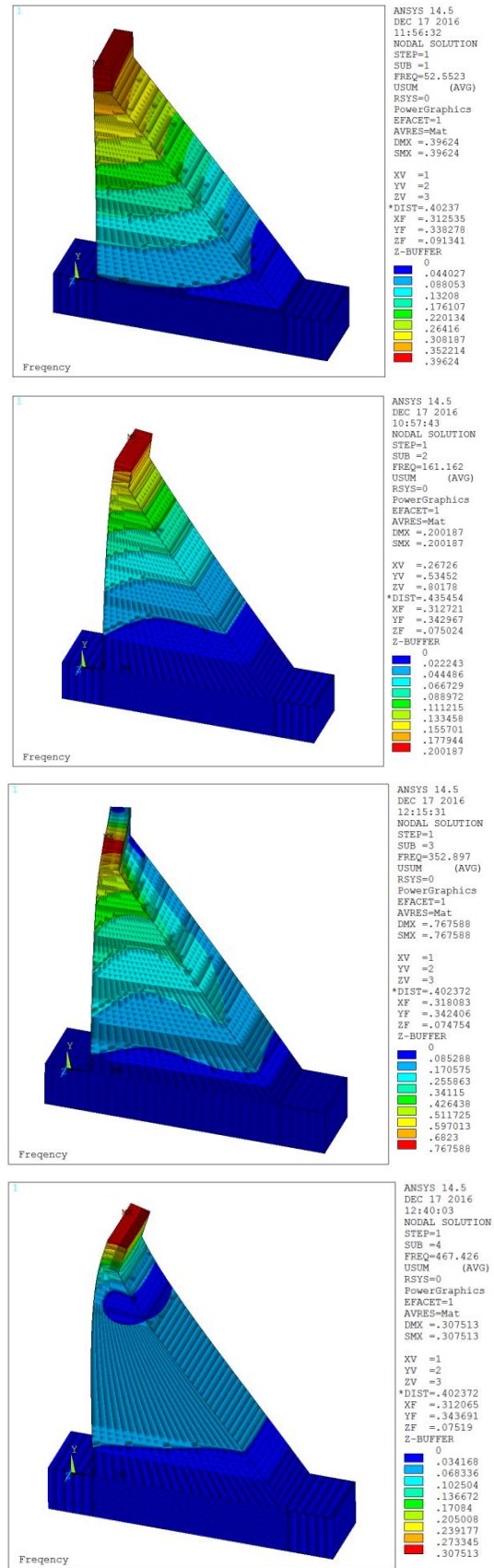


Fig. 29 Displacement vector contour images of all nodes under first four order natural frequencies

Table 2 Natural Frequencies Comparison among PCB accelerometer, FEM, and CPSM

Order	1 <sup>st</sup>	2 <sup>nd</sup>	3 <sup>rd</sup>	4 <sup>th</sup>	5 <sup>th</sup>
PCB (Hz)	49.84	150.18	317.98	395.95	525.17
CPSM (Hz)	49.77	150.22	317.47	461.15	487.05
FEM (Hz)	52.55	161.13	352.90	467.43	499.65
Relative Error (CPSM vs. PCB)	0.13%	0.03%	0.16%	14.14%	7.83%
Relative Error (CPSM vs. FEM)	5.29%	0.60%	10.04%	1.34%	2.52%
Order	6 <sup>th</sup>	7 <sup>th</sup>	8 <sup>th</sup>	9 <sup>th</sup>	10 <sup>th</sup>
PCB (Hz)	649.83	840.94	1059.62	1150.25	1287.98
CPSM (Hz)	650.27	859.56	1040.19	1135.71	1195.15
FEM (Hz)	680.37	909.69	997.58	1103.51	1284.00
Relative Error (CPSM vs. PCB)	0.07%	2.17%	1.87%	1.28%	7.77%
Relative Error (CPSM vs. FEM)	4.42%	5.51%	4.27%	2.92%	6.92%

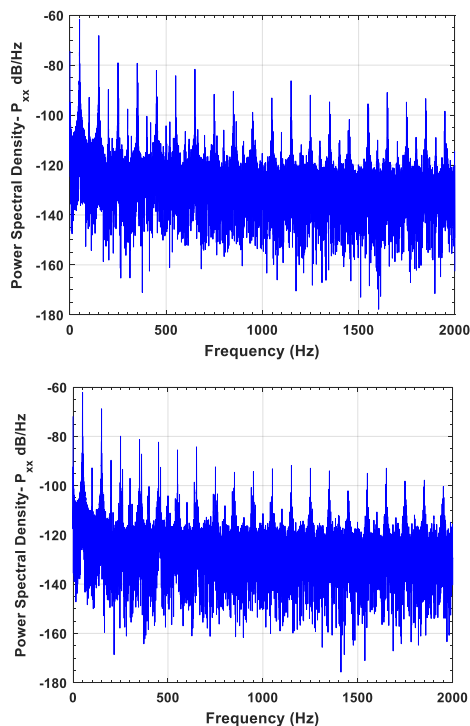


Fig. 30 PSD and Identified Natural Frequencies by PCB and CPSM

#### 4. Conclusions

Three major experiments are presented in the paper to assess the application of CPSMs in four different areas. The first, frequency properties obtained from CPSM and the comparison between them and the input signal properties, second, using CPSMs to get the attenuation function under certain excited signal, third, estimate the concrete strength

during early age and finally, comparing modal parameters of the same structure by using PCBs, CPSMs and finite element analysis.

Assessment was made by comparing the frequencies between excited linearly chirp signal and CPSM acquired signal. Fast Fourier Transform was applied to transfer the signal from time series to frequency domain. The power spectral density of both chirp signal and CPSM acquired signal were generated and compared. Results found that frequencies with higher densities locate in the same range. The PSD for CPSM acquired signal had lower value comparing to chirp signal due to the mixed noise.

Based on the embedded CPSMs in the concrete block and through the excited signal analysis, the signal magnitude attenuation function was obtained. The magnitudes for the sweeping frequencies had an exponential relationship with different frequencies. In general, in the certain frequency range, the higher the frequency the higher the magnitude of acquired signal.

Two CPSMs embedded into the concrete during hydration to excite and acquire signal in a certain time series. Assumptions were made by assuming, (1) the compressive wave propagated inside concrete as one-dimensional wave, and (2) concrete to be elasticity after approximately 7 days. Regardless of the earlier ages (1-6) (viscoelasticity) in which the damping of wave propagation is very big, the CPSM acquired signal magnitude was decreasing along with concrete solidification. CPSM acquired signal magnitude would decrease exponentially along with concrete solidification. Therefore, concrete strength could be estimated by considering the CPSM acquired signal amplitude.

Modal analysis was also performed to extract the modal parameter of the designed structure by using PCBs accelerometer, CPSMs and FEM analysis. The first ten order modal parameters were extracted through

experimental modal analysis by using both PCB acquired, CPSM acquired signals and FEM. PCB accelerometer were manufactured with regulations which were used as comparison and evaluation of CPSMs. Modal analysis results showed that CPSM acquired signal extracted modal natural frequencies agreed very well with PCBs acquired signal extracted modal natural frequencies. The extracted natural frequencies from both CPSMs had relative small error (2%) comparing to the ones extracted from PCBs. Additionally, the differences between CPSMs extracted model frequency had a relative small error (~5%) as well. The constructed CPSM is applicable for monitoring of civil structures.

## Acknowledgments

The first author would thank Dr. Huaizhi Su for his support in College of Water Conservancy and Hydropower Engineering at Hohai University during his M.S. study.

## References

- Aktan, A.E., Helmicki, A.J. and Hunt, V.J. (1998), "Issues in health monitoring for intelligent infrastructure", *Smart Mater. Struct.*, **7**(5), 674.
- Achenbach, J. (2012), *Wave Propagation in Elastic Solids (Vol. 16)*. Elsevier, Amsterdam, Netherlands.
- Bahei-El-Din, Y.A., Saleh, A.M., and Talaat, M.M. (2003), "Electro-mechanical impedance technique for health monitoring of concrete structures", *J. Eng. Appl. Sci. Cairo*, **50**(6), 1111-1124.
- Bernard, O., Ulm, F.J. and Lemarchand, E. (2003), "A multiscale micromechanics-hydration model for the early-age elastic properties of cement-based materials", *Cement Concrete Res.*, **33**(9), 1293-1309.
- Brigham, E.O. and Brigham, E.O. (1974), *The fast Fourier transform (Vol. 7)*. Englewood Cliffs, NJ: Prentice-Hall.
- Caicedo, J.M. (2011), "Practical guidelines for the natural excitation technique (NExT) and the eigensystem realization algorithm (ERA) for modal identification using ambient vibration", *Exper. Techniques*, **35**(4), 52-58.
- Chang, P.C., Flatau, A. and Liu, S.C. (2003), "Review paper: health monitoring of civil infrastructure", *Struct. Health Monit.*, **2**(3), 257-267.
- Chang, K.C. and Kim, C.W. (2016), "Modal-parameter identification and vibration-based damage detection of a damaged steel truss bridge", *Eng. Struct.*, **122**, 156-173.
- Chase, J.G., Barroso, L.R. and Hwang, K.S. (2004), "LMS-based structural health monitoring methods for the ASCE benchmark problem", *Proceedings of the American Control Conference 2004*, Boston, June.
- Clayton, E.H., Qian, Y., Orjih, O., Dyke, S.J., Mita, A. and Lu, C. (2006), "Off-the-shelf modal analysis: Structural health monitoring with motes", *Proceedings of the 24th International Modal Analysis Conference*. St. Louis, 2006, January.
- Doebbling, S.W., Farrar, C.R., Prime, M.B. and Shevitz, D.W. (1996), *Damage Identification and Health Monitoring of Structural and Mechanical Systems from Changes in their Vibration Characteristics: A Literature Review (No. LA-13070-MS)*, Los Alamos National Lab., NM, United States.
- Gentile, C., Saisi, A., and Cabboi, A. (2015), "Structural identification of a masonry tower based on operational modal analysis". *Int. J. Architect. Heritage*, **9**(2), 98-110.
- Gu, H., Song, G., Dhonde, H., Mo, Y.L. and Yan, S. (2006), "Concrete early-age strength monitoring using embedded piezoelectric transducers", *Smart Mater. Struct.*, **15**(6), 1837.
- Guo, H., Xiao, G., Mrad, N. and Yao, J. (2011), "Fiber optic sensors for structural health monitoring of air platforms", *Sensors*, **11**(4), 3687-3705.
- Giurgiutiu, V. (2007), *Structural Health Monitoring: with Piezoelectric Wafer Active Sensors*, Academic Press, Massachusetts, U.S.
- Haranki, B. (2009), "Strength, modulus of elasticity, creep and shrinkage of concrete used in Florida", Ph.D. Dissertation, University of Florida, Gainesville.
- Hearn, G. and Testa, R.B. (1991), "Modal analysis for damage detection in structures", *J. Struct. Eng. - ASCE*, **117**(10), 3042-3063.
- Ibrahim, S.R. and Mikulcik, E.C. Mikulcik (1973), "A time domain modal vibration test technique", *Shock Vib. Bul.*, **43**, 21-37.
- Ibrahim, S.R. and Pappa, R.S. (1982), "Large modal survey testing using the Ibrahim time domain identification technique", *J. Spacecraft Rockets*, **19**(5), 459-465.
- James III, G.H., Carne, T.G. and Lauffer, J.P. (1993), *The Natural Excitation Technique (NExT) for Modal Parameter Extraction from Operating Wind Turbines (No. SAND-92-1666)*. Sandia National Labs., Albuquerque, NM (United States).
- Leung, C.K., Wan, K.T., Inaudi, D., Bao, X., Habel, W., Zhou, Z., and Imai, M. (2015), "Review: optical fiber sensors for civil engineering applications", *Mater. Struct.*, **48**(4), 871-906.
- Noguchi, T., Tomosawa, F., Nemati, K.M., Chiaia, B.M. and Fantilli, A.P. (2009), "A practical equation for elastic modulus of concrete", *ACI Struct. J.*, **106**(5), 690.
- Park, G., Cudney, H.H., and Inman, D.J. (2000), "Impedance-based health monitoring of civil structural components", *J. Infrastruct. Syst.*, **6**(4), 153-160.
- Prashant, S.W., Chougule, V.N. and Mitra, A.C. (2015), "Investigation on modal parameters of rectangular cantilever beam using Experimental modal analysis", *Mater. Today: Proceedings*, **2**(4), 2121-2130.
- Quinn, A. (2010), *Digital Signal Processing using MATLAB (Vol. 14)*. John Wiley & Sons, New Jersey.
- Roy, S., Ladpli, P. and Chang, F.K. (2015), "Load monitoring and compensation strategies for guided-waves based structural health monitoring using piezoelectric transducers", *J. Sound Vib.*, **351**, 206-220.
- Song, G., Gu, H., Mo, Y.L., Hsu, T.T.C. and Dhonde, H. (2007), "Concrete structural health monitoring using embedded piezoceramic transducers", *Smart Mater. Struct.*, **16**(4), 959.
- Song, G., Gu, H. and Mo, Y.L. (2011), "Piezoceramic-based smart aggregate for unified performance monitoring of concrete structures". *U.S. Patent No. 7,987,728*. Washington, DC: U.S. Patent and Trademark Office.
- Stoica, P. and Moses, R.L. (2005), *Spectral Analysis of Signals (Vol. 452)*. Upper Saddle River, NJ: Pearson Prentice Hall.
- Su, H., Zhang, N., Yang, M. and Cai, S. (2014), Testing device capable of identifying natural vibration frequency of hydraulic concrete structure, Chinese patent CN203432772 U, Nanjing, China.
- Su, H., Zhang, N., Yang, M., Wen, Z. and Xie, W. (2015), "Experimental study on natural vibration frequency identification of hydraulic concrete structure using concrete piezoceramic smart module", *J. Vibroengineering*, **17**(7).
- Su, H., Zhang, N., Wen, Z. and Li, H. (2016), "Experimental study on obtaining hydraulic concrete strength by use of concrete piezoelectric ceramic smart module pairs", *J. Intel. Mat. Syst. Str.*, **27**(5), 666-678.
- Tennyson, R.C., Mufti, A.A., Rizkalla, S., Tadros, G. and Benmokrane, B. (2001), "Structural health monitoring of

- innovative bridges in Canada with fiber optic sensors”, *Smart Mater. Struct.*, **10**(3), 560.
- Tomosawa, F. and Noguchi, T. (1993), “Relationship between compressive strength and modulus of elasticity of high-strength concrete”, *Proceedings of the 3rd International Symposium on Utilization of High-Strength Concrete*, Lillehammer, June.
- Xu, D., Banerjee, S., Wang, Y., Huang, S. and Cheng, X. (2015), “Temperature and loading effects of embedded smart piezoelectric sensor for health monitoring of concrete structures”, *Constr. Build. Mater.*, **76**, 187-193.
- Zhang, X. and Jia, Y. (2005), “A soft decision based noise cross power spectral density estimation for two-microphone speech enhancement systems”, *Proceedings of the International Conference on Acoustics, Speech, and Signal Processing*, Philadelphia, March.

HJ